

Cold Plasma Wave Analysis in Magneto-Rotational Fluids

M. Sharif ^{1*} and Umber Sheikh ²

¹ Department of Mathematics, University of the Punjab,
Quaid-e-Azam Campus Lahore-54590, Pakistan.

² Department of Applied Sciences,
National Textile University Faisalabad-37610, Pakistan

Abstract

This paper is devoted to investigate the cold plasma wave properties. The analysis has been restricted to the neighborhood of the pair production region of the Kerr magnetosphere. The Fourier analyzed general relativistic magnetohydrodynamical equations are dealt under special circumstances and dispersion relations are obtained. We find the x -component of the complex wave vector numerically. The corresponding components of the propagation vector, attenuation vector, phase and group velocities are shown in graphs. The direction and dispersion of waves are investigated.

Keywords: 3+1 formalism, GRMHD, Kerr planar analogue, cold plasma, normal and anomalous dispersion.

PACS numbers: 95.30.Qd, 95.30.Sf, 04.30.Nk

1 Introduction

Einstein's general theory of relativity describes gravity as a curvature of spacetime caused by the presence of matter. Most massive physical objects

*msharif@math.pu.edu.pk

like black holes distort the geometry of spacetime by their immense gravity. The accretion disk around a rotating black hole (most physical in nature) is always filled with charged plasma due to the pair production in this region. This charged plasma creates an external magnetic field around the black hole (the region containing this field is termed as magnetosphere in literature) and is governed by the general relativistic magnetohydrodynamical (GRMHD) equations. The intrinsic angular momentum of the black hole intends the surrounding plasma to act as a magneto-rotational fluid. The black hole spin modifies the rotation of the plasma which flows in the form of an MHD wind. When this wind is perturbed analytically, GRMHD waves are formed. These waves propagate to transmit information in the magnetosphere. They also help us to detect whether the energy extraction is allowed by the plasma state in the magnetosphere.

There is a large body of literature available [1]-[9] about the perturbations and GRMHD waves in the regime of the Schwarzschild black hole. The study of rotating black holes has been an interesting subject since they lie in the hearts of active galaxies [10]. Blandford and Znajek [11] discussed the possibility of an electromagnetically driven wind from the rotating black hole. Takahashi et al. [12] discussed the MHD inflow and the extraction of energy in the form of jets.

In general relativity, different observers generally experience distinct time measures. In 1962, an attempt was made by Arnowitt et al. [13] who quantized the gravitational field by a specific foliation (now called ADM 3+1 formalism). Thorne and Macdonald [14]-[15] used the ADM 3+1 split to bridge the gap between the black hole electrodynamics and that of flat space electrodynamics. The formalism was taken over by Holcomb and Tajima [16] and Dettmann et al. [17] to discuss the quantum description of plasma including electromagnetic waves in FRW metric. Buzzi et al. [18] used this access to investigate the wave phenomenon near the Schwarzschild event horizon by using two component plasma. Recently, Sharif and Sheikh [19]-[22] worked on the properties of cold and isothermal plasmas living in the neighborhood of the Schwarzschild event horizon. Komissarov [23] discussed Blandford-Znajek monopole solution for black hole electrodynamics using 3+1 formalism. Khanna [24] derived the generalized Ohm's law in 3+1 split.

The energy can be extracted from the ergosphere via a process first proposed by Penrose [25]: a particle entering the ergosphere can split in two in such a way that one fragment falls into the hole, but the other leaves the ergosphere with more energy than the original particle. The extra energy comes

from the hole itself. Leiter and Kafatos [26] discussed the Penrose pair production in massive Kerr black hole's ergosphere. Kafatos [27] discussed the gamma ray observations from Penrose powered black holes. Koide et al. [28] modeled the GRMHD behavior of plasma flowing into the rotating black hole in a magnetic field and showed (using numerical simulations) that energy of the spinning black hole can be extracted magnetically. Another way of extracting black hole's spin energy is the form of super-radiance. Kokkotas and Schmidt [29] discussed quasi normal modes for black holes and relativistic stars. They have also discussed the w-waves or gravitational wave modes in these scenarios. Furuhashi and Nambu [30] discussed the super-radiance in charged Kerr spacetime by numerically solving the Klein-Gordon equation as an eigen value problem. Zeldovich [31] considered the waves scattering by a rotating conducting cylinder. They proved that Kerr geometry displays super-radiance. Zhang [32]-[33] formulated the black hole theory for stationary symmetric GRMHD with its applications in Kerr geometry. He showed (taking the specific values of the angular frequency and the x -component of the wave vector) that the cold plasma allows the outflow of energy flux. Recently, Sharif and Sheikh [34]-[37] extended this work to cold and isothermal plasmas by investigating the real wave numbers. They verified the results given by Zhang [33]. This work partially helps to answer the question of energy extraction.

In this paper, we shall discuss the cold plasma wave properties by calculating complex wave numbers. This provides an alternative to verify the results obtained in [37]. We have considered the Fourier analyzed perturbed GRMHD equations for the planar analogue of the Kerr metric. These equations lead to the dispersion relation and consequently the x -component of the complex wave vector for the cold plasma. This complex x -component can be split into x -components of the propagation factor (real part) and attenuation factor (imaginary part). Further, we evaluate the x -components of the phase and group velocities etc. near the pair production region. These quantities would help us to understand the modes of dispersion.

The layout of this paper is as follows. Section 2 provides the description of spacetime near the pair production region with some assumptions. Section 3 consists of the background flow assumptions and related quantities used in specification and interpretation of results. In Section 4, we Fourier analyze the GRMHD equations for the cold plasma. Section 5 is devoted to the numerical solutions of the dispersion relation. It also includes figures and related discussion. The observable quantities are given which help us to judge

the waves properties more efficiently. We shall conclude this discussion in Section 6.

2 Description of Model Spacetime

The most general line element in 3+1 formalism can be written as

$$ds^2 = -\alpha^2 dt^2 + \gamma_{ij}(dx^i + \beta^i dt)(dx^j + \beta^j dt), \quad (2.1)$$

where α is the lapse function, β^i are the components of shift vector and γ_{ij} are the components of spatial metric. All these quantities are functions of time and space coordinates.

We consider the planar analogue of the Kerr metric [34]

$$ds^2 = -dt^2 + (dx + \beta(z)dt)^2 + dy^2 + dz^2. \quad (2.2)$$

The directions z , x and y are the analogue of the Kerr's radial r , axial ϕ and poloidal θ directions respectively whereas t represents the time coordinate. Utilizing coordinate freedom, the lapse function is set to unity without loss of generality. This has been done to avoid complications which arise due to the presence of horizon and hence, the red-shifts. The rotation of the black hole imposes a shift vector which is obvious from Eq.(2.2). The value of the shift function β (analogue to the Kerr-type gravitomagnetic potential) decreases monotonically from 0 ($z \rightarrow \infty$) to some constant value ($z \rightarrow -\infty$). Equation (2.2) shows that our assumed β is $\beta(z) \equiv \beta(z)\mathbf{e}_x$ which derives an MHD wind and extract translational energy analogous to the rotational energy of the Kerr metric. The plasma particles, created at $z = 0$ (pair production region), are then driven up to relativistic velocities by magnetic-gravitomagnetic coupling, as they flow off to "infinity" ($z = +\infty$) and down towards the "event horizon" ($z = -\infty$).

Our scenario is based on the pair production region and its surrounding plasma. Thus we are interested in the magnetospheric plasmas rotating in the 2-D fashion i.e. in (zx -plane). The shift is restricted to be dependent on only one dimension. It may depend on the other dimensions which obviously make the analysis tough but more general. The shift is the effect of black hole rotation, of course. The plasma is being produced in the pair production region (electron-positron pair production holds and at $z = 0$ in our scenario) outflows from the region towards the event horizon which lies at $z = -\infty$ and

towards the outer end of the magnetosphere (the end away from the event horizon). The plasma produced in the pair production region falls out from the region. This outflow disturbs the neighboring magnetospheric plasma in the form of waves. The region $z = 0$ is not a physical singularity but the region where particle-antiparticle pairs are produced from the vacuum energy. Since the out flowing plasma is moving in the xz -plane, so it will absolutely disturb the outer plasma in the same plane.

This spacetime requires a fiducial reference observer (FIDO) (analogous to the zero angular momentum observer of the 3+1 split of the Kerr spacetime), the one with four-velocity perpendicular to the hypersurfaces of constant time t . The geometrized units will be used throughout the paper.

3 Plasma Flow and Relative Assumptions

We consider a rotating background which is assumed to be filled with cold plasma admitting the following equation [33]

$$\mu = \frac{\rho}{\rho_0} = \text{constant}, \quad (3.1)$$

where μ , ρ_0 and ρ are the specific enthalpy, rest and moving mass densities of the fluid respectively. This shows that the plasma has vanishing thermal pressure and thermal energy. Thus the cold plasma particles are moving along timelike geodesics of the spacetime (2.2).

The rotating fluid's four-velocity and magnetic field measured by our FIDO can be described by spatial vector fields lying in xz -plane

$$\mathbf{V} = V(z)\mathbf{e}_x + u(z)\mathbf{e}_z, \quad \mathbf{B} = B\{\lambda(z)\mathbf{e}_x + \mathbf{e}_z\}, \quad (3.2)$$

where B is a constant.

For the stationary symmetric background, the relationship between x and z components of the velocity vector for the spacetime (2.2) can be written as [33]

$$V = C + \lambda u, \quad (3.3)$$

where $C \equiv \beta + V_F$ is the normalized shift and V_F is an integration constant. Further, the mass conservation law in three-dimensional hypersurface is

$$\alpha \rho_0 \gamma u = A \text{ (constant)}, \quad (3.4)$$

where $\gamma = \frac{1}{\sqrt{1-u^2-V^2}}$ is the Lorentz factor.

We take the assumptions $V_F = 1$, $\beta = \tanh(z) - 1$ for simplifications. It is important to note that our assumed β is continuous across $z = 0$ (i.e., the pair production region). This shift may not be valid for the near horizon. The expansion of shift vector β implies that this vector is directly proportional to the dimensionless angular momentum $J = \frac{a}{M}$ of the black hole and inversely proportional to the radius of the black hole. Thus the spin of the black hole can be expressed by the following relation [15]

$$\beta = \frac{2JM}{(r')^3}(ye_x - xe_y) + O\left(\frac{1}{r'^4}\right),$$

where $r' = \sqrt{x^2 + y^2 + z^2}$. This β is involved in all the dispersion relations. As the function β changes, the value of the dispersion relation (i.e., the relationship between the wave number and angular frequency) changes. In this work, we consider only the propagation which changes due to change in z and hence the change in β .

According to these assumptions, the MHD flow is intended to model a wind flowing out of the ergosphere of a Kerr black hole and also an accretion flow down to the horizon, both originated at the pair production region, i.e., $z = 0$. At the pair production region, $\beta = -1$. The renormalized shift vector is $C = \beta + V_F$ where $V_F = 1$, is a flow constant. There is no flow at $z = 0$, thus $C = \beta + V_F = -1 + 1 = 0$ at $z = 0$.

Our assumed plasma's magnetic field having a variable x -component λB with variable λ depends on the variable z . The plasma is frozen-in to the B -field and we have assumed an adiabatic flow. For simplification, we have also taken $\lambda = 1$, i.e., the x -component of the magnetic field becomes constant and leads to a constant unperturbed magnetic field. When we apply these values to Eq.(3.3) and then substitute the resulting value of V in Eq.(3.4) with the simplification $A/\rho_0 = 1$ (as done in [34]-[36]), we obtain the following pairs of velocity components.

$$u_1 = -\frac{1}{3}\tanh(z) - \frac{1}{3}l, \quad V_1 = \frac{2}{3}\tanh(z) - \frac{1}{3}l, \quad (3.5)$$

$$u_2 = -\frac{1}{3}\tanh(z) + \frac{1}{3}l, \quad V_2 = \frac{2}{3}\tanh(z) + \frac{1}{3}l, \quad (3.6)$$

where $l = \sqrt{3 - 2\tanh^2(z)}$. The corresponding Poynting vector, then, takes the form

$$\mathbf{S} = \frac{1}{4\pi}\mathbf{E} \times \mathbf{B} = 2\tanh(z)(\mathbf{e}_x - \mathbf{e}_z). \quad (3.7)$$

These assumptions lead to a rotating black hole magnetospheric fluid which admits a constant external magnetic field. The fluid is moving with a velocity \mathbf{V} in the magnetosphere. The gravitomagnetic waves and pair of particles are produced in the $z = 0$ region. The energy extraction from the black hole is possible if the medium allows the waves and particles to pass through it and move out of the magnetosphere. The gravitomagnetic waves transform information within plasma. If the medium, in the region under consideration, allows the waves to move normally, these waves can get out of the magnetosphere. This can be well understood by investigating properties of the waves in this region.

The plasma flow in the magnetosphere is perturbed due to gravity and rotation of the black hole. This flow is characterized by fluid's density ρ , velocity \mathbf{V} and magnetic field \mathbf{B} . The linear perturbations will be in xz -plane and thus are dependent on x , z and t . The perturbed variables take the following form

$$\rho = \rho^0 + \rho\tilde{\rho}, \quad \mathbf{V} = \mathbf{V}^0 + \mathbf{v}, \quad \mathbf{B} = \mathbf{B}^0 + B\mathbf{b}, \quad (3.8)$$

where unperturbed quantities are denoted by the superscript zero. Further, the dimensionless notations $\tilde{\rho}$, \mathbf{v} and \mathbf{b} can be expressed as

$$\begin{aligned} \tilde{\rho} &\equiv \frac{\delta\rho}{\rho} = \tilde{\rho}(t, x, z), \\ \mathbf{v} &\equiv \delta\mathbf{V} = v_x(t, x, z)\mathbf{e}_x + v_z(t, x, z)\mathbf{e}_z, \\ \mathbf{b} &\equiv \frac{\delta\mathbf{B}}{B} = b_x(t, x, z)\mathbf{e}_x + b_z(t, x, z)\mathbf{e}_z. \end{aligned} \quad (3.9)$$

The perturbations are assumed to be harmonic, i.e., of the form $\delta = e^{-i(\omega t - k_x x - k_z z)}$ (having sinusoidal dependence on t , x and z).

$$\begin{aligned} \tilde{\rho}(t, x, z) &= c_1\delta, \quad v_x(t, x, z) = c_2\delta, \quad v_z(t, x, z) = c_3\delta, \\ b_x(t, x, z) &= c_4\delta, \quad b_z(t, x, z) = c_5\delta, \end{aligned} \quad (3.10)$$

where c_1 , c_2 , c_3 , c_4 , c_5 are arbitrary constants, k_x and k_z are the x and z -components of the wave vector $\mathbf{k} = (k_x, 0, k_z)$ and ω is angular frequency of the wave.

4 Fourier Analyzed Perturbed GRMHD Equations

The perfect GRMHD equations for the Kerr planar analogue (Eq.(2.2)) is given by Eqs.(2.4)-(2.8) of [35]. Substituting the value of rest-mass density from Eq.(3.1), we obtain their specific form for the cold plasma. The insertion of perturbed values from Eq.(3.8) and then from Eq.(3.9) give the component form of these equations. This is the same procedure as given in [19] and [34].

Since the perturbed variables have harmonic dependence on x , z and t , hence Eq.(3.10) is used and the following Fourier analyzed form is obtained.

$$\iota k_z c_2 - (\iota k_z \lambda + \lambda') c_3 - c_4 (\iota k_z u - \iota \omega + u') + c_5 (m \iota k_z + m') = 0, \quad (4.1)$$

$$\iota k_x c_2 - \iota k_x \lambda c_3 + \iota c_5 \{m k_x + k_z u - \omega\} = 0, \quad (4.2)$$

$$k_x c_4 = -k_z c_5, \quad (4.3)$$

$$\begin{aligned} & c_1 \iota \{-\omega + m k_x + u k_z\} + c_2 [-\iota w \gamma^2 V + \iota k_z \gamma^2 u V + \iota k_x q + \\ & \gamma^2 u \{(1 + 2\gamma^2 V^2) V' + 2\gamma^2 u V u'\}] + c_3 [-\iota (\omega + \beta k) \gamma^2 u \\ & + \iota k_z r + \iota k_x \gamma^2 u V + 2\gamma^4 u^2 V V' - (1 - 2\gamma^2 u^2) r \frac{u'}{u}] = 0, \end{aligned} \quad (4.4)$$

$$\begin{aligned} & c_1 \rho \gamma^2 u \{q V' + \gamma^2 u V u'\} + c_2 [-\iota w \{\rho \gamma^2 q + s\} + \iota y \{\rho \gamma^2 q - s\} \\ & + \rho \gamma^4 u \{(1 + 4\gamma^2 V^2) u u' + 4q V V'\}] + c_3 [-\iota w \{\rho \gamma^4 u V - \lambda s\} \\ & + \iota y \{\rho \gamma^4 u V + \lambda s\} + \rho \gamma^2 \{(1 + 2\gamma^2 u^2)(1 + 2\gamma^2 V^2) \\ & - \gamma^2 V^2\} V' + 2\gamma^2 (1 + 2\gamma^2 u^2) u V u'] + u \lambda' s] + s c_4 \{-\iota k_z (1 - u^2) \\ & + u u'\} + s c_5 \{-\lambda' - u m' + \iota k_x (1 - V^2) - 2\iota u V k_z\} = 0, \end{aligned} \quad (4.5)$$

$$\begin{aligned} & c_1 \gamma^2 \rho [u \{r u' + \gamma^2 V u V'\} - V \beta'] + c_2 [-\iota w \{\rho \gamma^4 u V - \lambda s\} \\ & + \iota y \{\rho \gamma^4 u V + \lambda s\} + \rho \gamma^2 \{\gamma^2 u^2 V' (1 + 4\gamma^2 V^2) - \beta' (1 + 2\gamma^2 V^2) \\ & + 2V \gamma^2 u u' (1 + 2\gamma^2 u^2)\}] + c_3 [-\iota \{\rho \gamma^2 (1 + \gamma^2 u^2) + \lambda^2 s\} w \\ & + \iota y \{\rho \gamma^2 r - \lambda^2 s\} + \rho \gamma^2 [u' (1 + \gamma^2 u^2) (1 + 4\gamma^2 u^2) \\ & + 2u V \gamma^2 \{m' + 2\gamma^2 u^2 V'\}] - s \lambda \lambda' u] + s c_4 \{\iota k_z \lambda (1 - u^2) \\ & + \lambda' - \lambda u u'\} + s c_5 \{2\lambda u V \iota k_z + \lambda u m' - \iota k_x \lambda (1 - V^2)\} = 0, \end{aligned} \quad (4.6)$$

where $m = V - \beta$, $q = 1 + \gamma^2 V^2$, $r = 1 + \gamma^2 u^2$, $s = \frac{B^2}{4\pi}$, $w = \omega + \beta k_x$ and $y = k_x V + k_z u$. Equation (4.3) gives the relation between k_x and k_z , i.e., $k_x = -\frac{c_5}{c_4} k_z$. We assume $c_4 = c_5$ yielding $k_x = -k_z$ which reduces our wave vector

to $\mathbf{k} = (k_x, 0, -k_x)$ with wave number $k = |\mathbf{k}| = \sqrt{2k_x^2}$. This assumption will make the set of equations easier to solve. The relaxation in this assumption may change the regions of normal and anomalous dispersion.

5 Numerical Solutions

When we solve the determinant of the coefficients of Eqs.(4.1), (4.2), (4.4)-(4.6) of constants (c_1, c_2, c_3, c_4, c_5) for the x -component of the wave vector, it gives a complex dispersion relation of the form:

$$\begin{aligned} & A_1(\omega, z)k_x^4 + A_2(\omega, z)k_x^3 + A_3(\omega, z)k_x^2 + A_4(\omega, z)k_x + A_5(\omega, z) \\ & + \iota\{B_1(\omega, z)k_x^5 + B_2(\omega, z)k_x^4 + B_3(\omega, z)k_x^3 + B_4(\omega, z)k_x^2 \\ & + B_5(\omega, z)k_x + B_6(\omega, z)\} = 0. \end{aligned} \quad (5.1)$$

This relation is quintic in k_x and cannot give exact solutions. Thus, we solve it numerically by using *Mathematica*, for the complex values of k_x . The assumption $k_x = -k_z$ implies that k_z is also a complex number. Thus the quantities given by Eq.(3.10) take the form

$$\sim e^{-\iota(\omega t - k_x x - k_z z)} = e^{-\iota(\omega t - k_{Rx}x - k_{Rz}z) - k_{Ix}x - k_{Iz}z},$$

where $k_x = k_{Rx} + \iota k_{Ix}$ and $k_z = k_{Rz} + \iota k_{Iz}$. The values k_{Rx} and k_{Rz} represent the x and z -components of the propagation factor from which we can obtain the x and z -components of the phase and group velocities whereas k_{Ix} and k_{Iz} represent the x and z -components of the attenuation factor.

We have considered the region $-5 \leq z \leq 5$ to analyze the wave properties of the cold plasma. The cold flow assumption indicates that the fluid has no viscosity and no heat conduction. This is indeed an ideal case but provides basis for the case of hot plasma, thus has its own importance. Perturbations themselves modify this assumption because we include the perturbations in the GRMHD equations for cold plasma. Since the flow variables u, V, λ have more variations near the pair production region, thus we have excluded the region $-1 < z < 1$ and solved the relation for rest of the region where these variables have small variation. Thus the region under consideration $-5 \leq z \leq 5$ is divided into two regions $-5 \leq z \leq -1$ and $1 \leq z \leq 5$ for which roots are numerically interpolated. The region $-5 \leq z \leq -1$ indicates the neighborhood of the pair production region towards the event horizon and the region $1 \leq z \leq 5$ shows the neighborhood of the pair production

region towards the outer end of the magnetosphere. We take the step-length 0.2 for z and ω and find the value of k_x at each point (z_i, ω_j) ($i = 1, \dots, 21$, $j = 1, \dots, 51$) of the mesh. Then by separating each root, we estimate the surface by numerical interpolation. The x -components of the propagation vector, attenuation vector, phase and group velocities can be evaluated from these interpolation functions.

We have obtained two velocities (given by Eqs.(3.5) and (3.6)) for our assumed plasma (i.e., rotating cold plasma with constant rest-mass density). For each velocity, Eq.(5.1) leads to five values of the x -component of the wave numbers. We display x -components of the propagation vector, attenuation vector, phase and group velocities and analyze the dispersion with respect to these quantities.

For the region towards the black hole horizon with the fluid flow velocity given by Eq.(3.5), we obtain one root for which the wave number is infinite at several values of z . Such a root is also found for the region towards the outer end of the magnetosphere ($z = \infty$) for the velocity components (Eq.(3.6)). These roots indicate that the waves are evanescent there which decreases with the passage of time. Thus the energy cannot pass through the region via waves and hence these cases are not interesting. For the velocity components (3.5), the dispersion relations obtained in the region towards the event horizon in the neighborhood of the pair production region are given by Figures 1-4. Figures 6-9 indicate the dispersion relations for the region towards the outer end of the magnetosphere. The dispersion relations related to the velocity components (3.6) for the region towards the event horizon are given by Figures 10-14. For the region towards the outer end of the magnetosphere, these relations are shown by Figures 15-18.

In Figures 1-4 and 10-14, the positive propagation factor shows that the waves are moving towards the pair production region whereas the negative propagation factor indicates that the waves are moving towards the event horizon. We see from Figures 6-9 and 15-18 that when the propagation factor is positive, the waves are moving towards the outer end of the magnetosphere whereas the negative propagation factor indicates that the waves are moving towards the pair production region. Table 1 indicates the regions of magnetosphere with the directed waves. The rest of the region contains random points of positive and negative propagation factor and thus the direction of waves changes at each point.

If the attenuation factor is increasing, it leads to the damping of waves whereas if this factor decreases, it indicates wave growth. Table 2 shows

| Figure No. | Region of waves moving towards the event horizon | Region of waves moving towards pair production region | Region of waves moving towards the outer end |
|------------|--|---|--|
| 1 | — | $-2.62 \leq z \leq -1^*$ | — |
| 2 | $-2 \leq z \leq -1$ | — | — |
| 3 | — | $-2 \leq z \leq -1$ | — |
| 4 | — | $-2.1 \leq z \leq -1$ | — |
| 5 | — | Entire Region | — |
| 6 | — | — | Entire Region* |
| 7 | — | — | Entire Region* |
| 8 | — | — | Entire Region* |
| 9 | — | — | Entire Region* |
| 10 | Entire Region | — | — |
| 11 | — | Entire Region | — |
| 12 | — | Entire Region* | — |
| 13 | — | Entire Region* | — |
| 14 | — | Entire Region | — |
| 15 | — | $1 \leq z \leq 2.7$ | — |
| 16 | — | — | $1 \leq z \leq 2.25^*$ |
| 17 | — | $1 \leq z \leq 2^*$ | — |
| 18 | — | — | Entire Region |

Table 1: Table indicating the direction of waves in respective regions.

the damping and growth of waves. The up-arrow in the table shows the increase whereas the down-arrow shows the decrease in respective quantity. The attenuation factor takes random values otherwise.

In a region where the phase velocity is greater than the group velocity, the waves are dispersed normally [38]-[39] whereas the group velocity greater than the phase velocity shows that the waves disperse anomalously. Table 3 shows the regions of normal and anomalous dispersion of waves in respective figures. Rest of the region contains random points of normal and anomalous dispersion.

We note that in all the tables star (*) means validity of the attribute to the whole region except for waves with negligible angular frequency.

| Figure No. | Regions of Wave Growth | Regions of Wave Damping |
|------------|---|---|
| 1 | $-1.6 \leq z \leq -1,^*$ $0.398 \leq \omega \leq 7.25$ as $\omega \uparrow$ and $z \downarrow$ | — |
| 2 & 3 | Random | Random |
| 4 | — | $-1.5 \leq z \leq -1$ as $\omega \uparrow$ and $z \downarrow$ |
| 5 | $0 \leq \omega \leq 0.23$ as $\omega \uparrow$ $1 \leq z \leq 1.4, 0.23 \leq \omega \leq 10$ as $z \uparrow$ | $1.4 \leq z \leq 5$ as $z \uparrow$ $1 \leq z < 1.4, 0 \leq \omega \leq 0.23$ as $z \uparrow$ |
| 6 | — | $1 \leq z \leq 2, 0.35 \leq \omega \leq 10$ as $z \uparrow$ and $\omega \downarrow$ $2 \leq z \leq 5, 0.35 \leq \omega \leq 10$ as $z \uparrow$ |
| 7 | — | As $z \uparrow^*$ |
| 8 | — | As $\omega \uparrow$ and $z \downarrow$ |
| 9 | $1.425 < z \leq 5, 0.2 \leq \omega \leq 10$ as $z \uparrow$ $1 \leq z \leq 5, 0 \leq \omega < 0.2$ as $z \uparrow$ | $1 \leq z \leq 1.425, 0.2 \leq \omega \leq 10$ as $z \uparrow$ |
| 10 | $-1.35 \leq z \leq -1$ as $ z \uparrow$ $1 \leq z \leq 2, 0.195 \leq \omega \leq 10$ as $z \uparrow$ | $-5 \leq z \leq -1.35$ as $ z \uparrow$ |
| 11 | $-1.35 \leq z \leq -1$ as $z \downarrow$ | $-5 \leq z \leq -1.35$ as $z \downarrow$ |
| 12 | As $ z \uparrow$ | As $\omega \uparrow$ |
| 13 | $z \downarrow$ and $\omega \uparrow$ | — |
| 14 | — | $-5 \leq z \leq -1, 0.175 \leq \omega \leq 10$ as $z \uparrow$ and $\omega \uparrow$ |
| 15 | $1.6 \leq z \leq 1.8, 0 \leq \omega \leq 0.195$ as $z \uparrow$ and $\omega \uparrow$ | $1 \leq z \leq 2, 0.195 \leq \omega \leq 10$ as $z \uparrow$ $1 \leq z \leq 1.6, 0 \leq \omega \leq 0.195$ as $z \uparrow$ and $\omega \uparrow$ $1.8 \leq z \leq 2, 0 \leq \omega \leq 0.195$ as $z \uparrow$ and $\omega \uparrow$ |
| 16 | $1.5 \leq z \leq 1.625$ | $1.0 \leq z \leq 1.5$ |
| 17 & 18 | Random | Random |

Table 2: Table indicating the regions of growth and damping of waves.

| Figure No. | Regions of Normal Dispersion | Regions of Anomalous Dispersion |
|------------|---|--|
| 1 | $-1.6 \leq z \leq -1, 0.1 \leq \omega \leq 7.25$ | — |
| 2 | — | $-2.15 \leq z \leq -1, 0 < \omega \leq 0.05$ |
| 3 | Random | Random |
| 4 | — | $-2 \leq z \leq -1$ |
| 5 | $1 \leq z \leq 1.25, 0 < \omega \leq 2$ $1.25 \leq z < 3, 0 < \omega \leq 1$ $3 \leq z \leq 5, 0 \leq \omega \leq 0.75$ | — |
| 6 | — | $2 \leq z \leq 5, 0.8 \leq \omega \leq 1,$ $1 \leq z \leq 4, 0.5 \leq \omega \leq 0.8,$ $1 \leq z \leq 5, 0 < \omega \leq 0.5$ |
| 7 | Entire region* | — |
| 8 | — | $0.2225 \leq \omega \leq 5$ |
| 9 | $\omega < 0.4025$ | — |
| 10 | $-5 \leq z \leq -4.2, 0 < \omega \leq 0.1$ | — |
| 11 | $-3 \leq z \leq -2.5, 0 < \omega \leq 0.4$ | $-5 \leq z \leq -3, 0 < \omega \leq 5$ $-2.5 \leq z \leq -1, 0 < \omega \leq 10$ |
| 12 | Random | Random |
| 13 | $-5 \leq z \leq -2, 0 < \omega \leq 0.2$ | $-5 \leq z \leq -1, 0.2 \leq \omega \leq 10$ $-2 \leq z \leq -1, 0.16 \leq \omega \leq 0.2$ |
| 14 | $-2 \leq z \leq -1, 0.1 \leq \omega \leq 0.39$ $-2 \leq z \leq -1, 0.41 \leq \omega \leq 0.5$ $-2.2 \leq z \leq -1, 0 < \omega \leq 0.08$ | — |
| 15 | — | $1.8 \leq z \leq 2, 0.002 \leq \omega \leq 0.003$ |
| 16 | $1 \leq z \leq 1.4, 2.5 \leq \omega \leq 10$ $1 \leq z \leq 1.4, 1 \leq \omega \leq 1.6$ $1 \leq z \leq 1.25, 1.6 \leq \omega \leq 2$ | — |
| 17 | $1.8 \leq z \leq 2, 0 \leq \omega \leq 0.00015$ | $1 \leq z \leq 1.5, 0 \leq \omega \leq 1.25$ |
| 18 | $1 \leq z \leq 1.45, 0 < \omega \leq 3.5$ | — |

Table 3: Table indicating the regions admitting normal and anomalous dispersion of waves.

6 Conclusion

This work is devoted to investigate the wave properties in the neighborhood of the pair production region. We have considered rotating cold plasma filled magnetosphere. The perturbations are assumed to be simple harmonic waves caused by the gravity influence as well as the rotation of the black hole. The determinant of the Fourier analyzed GRMHD equations is solved to obtain the x -component of the wave vector which is found to be a complex number. This has been done numerically for the two values of the velocity of the magneto-rotational fluid obtained in Section 3. The relation between the x and z -components of the wave vector is $k_x = -k_z$. This indicates that if we can have information about k_x and its corresponding quantities, we can infer the results for the waves moving along z -axis.

The summary of these results can be expressed as follows:

The propagation and attenuation factors take random values far from the pair production region in Figures 1-4, 15-18. The propagation factor increases with increasing angular frequency in Figures 6-9, 11-14. This gives the increment in propagation of waves along x -axis with the increment in angular frequency. It is observed in Figures 5-14 that the phase and group velocities take their extreme values (either maximum or minimum) near the pair production region. Thus the pair production region allows the waves to take extreme values near it.

In most of the figures, the region in the extreme neighborhood of the pair production region admits the waves to pass through (normal dispersion) which indicates that the waves can pass through this region. Anomalous dispersion in the extreme neighborhood of the pair production region in Figures 2, 4, 6, 8, 11, 13 and 17. In the region of anomalous dispersion, the phase velocity is less than the group velocity, so the waves cannot carry energy alongwith. Most of the figures show random dispersion of waves in the far regions of the pair production region.

Figure 7 shows normal dispersion of waves throughout the region which indicates that the waves can move towards the outer end of the magnetosphere. This verifies the result given by Zhang [33] and Sheikh [37] that cold plasma allows outflow of energy flux from the pair production region.

It would be worth exploring to check these properties by taking a hot plasma in a rotating magnetosphere.

References

- [1] Regge, T. and Wheeler, J.A.: Phys. Rev. **108**(1957)1063.
- [2] Zerilli, F.: Phys. Rev. **D2**(1970)2141; Phys. Rev. Lett. **24**(1970)737.
- [3] Price, R.H.: Phys. Rev. **D5**(1972)2419; ibid 2439.
- [4] Hanni R.S. and Ruffini, R.: Phys. Rev. **D8**(1973)3259.
- [5] Wald, R.M.: Phys. Rev. **D10**(1974)1680.
- [6] Mashhoon, B.: Phys. Rev. **D10**(1974)1059.
- [7] Sakai, J. and Kawata, T.: J. Phys. Soc. Jpn. **49**(1980)747.
- [8] Gosh, P: Mon. Not. R. Astron. Soc. **315**(2000)89.
- [9] Moortgat, J. and Kuijpers, J.: Mon. Not. R. Astron. Soc. **368**(2006)1110.
- [10] Lynden-Bell, D.: Nature **223**(1969)690.
- [11] Blandford, R.D. and Znajek, R.L.: Mon. Not. R. Astron. Soc. **179**(1977)433.
- [12] Takahashi, M., Nitta, S., Tatematsu, Y. and Tomimatsu, A.: Astrophys. J. **363**(1990)206.
- [13] Arnowitt, R., Deser, S. and Misner, C.W.: *Gravitation: An Introduction to Current Research* ed. Witten, L. (Wiley, New York, 1962); gr-qc/0405109v1.
- [14] Thorne, K.S. and Macdonald, D.A.: Mon. Not. R. Astron. Soc. **198**(1982)339; ibid **198**(1982)345.
- [15] *Black Holes: The Membrane Paradigm* eds. Thorne, K.S., Price, R.H. and Macdonald, D.A. (Yale University Press, New Haven, 1986).
- [16] Holcomb, K.A. and Tajima, T.: Phys. Rev. **D40**(1989)3809.
- [17] Dettmann, C.P., Frankel, N.E. and Kowalenko, V.: Phys. Rev. **D48**(1993)5655.

- [18] Buzzi, V., Hines, K.C. and Treumann, R.A.: Phys. Rev. **D51**(1995)6663; ibid 6677.
- [19] Sharif, M. and Sheikh, U.: Gen. Relat. Gravit. **39**(2007)1437; ibid 2095.
- [20] Sharif, M. and Sheikh, U.: Int. J. Mod. Phys. **A23**(2008)1417.
- [21] Sharif, M. and Sheikh, U.: J. Korean Phys. Soc. **52**(2008)152.
- [22] Sharif, M. and Sheikh, U.: J. Korean Phys. Soc. **53**(2008)2198.
- [23] Komissarov, S.S.: Mon. Not. R. Astron. Soc. **336**(2002)759.
- [24] Khanna, R.: Mon. Not. R. Astron. Soc. **294**(1998)673.
- [25] Penrose, R.: Riv. Nuovo Cimento **1**(1969)252.
- [26] Leiter, D. and Kafatos, M.: Astrophys. J. **226**(1978)32.
- [27] Kafatos, M.: Astrophys. J. **236**(1980)99.
- [28] Koide, S., Shibata, K., Kudoh, T. and Meier, D.L.: Science **295**(2002)1688.
- [29] Kokkotas, K. and Schmidt, B.: Liv. Rev. Rel **2**(1999)2.
- [30] Furuhashi, H. and Nambu, Y.: Prog. Theor. Phys. **112**(2004)983-995.
- [31] Zel'dovich, Y. B.: Zh. Eksp. Teor. Fiz. **62**(1972)2076 (Sov. Phys. JETP **35** (1972)1085).
- [32] Zhang, X.-H.: Phys. Rev. **D39**(1989)2933.
- [33] Zhang, X.-H.: Phys. Rev. **D40**(1989)3858.
- [34] Sharif, M. and Sheikh, U.: J. Korean Phys. Soc. (2009, to appear).
- [35] Sharif, M. and Sheikh, U.: Class. Quantum Grav. **24**(2007)5495.
- [36] Sharif, M. and Sheikh, U.: Canadian J. Phys. (2009, to appear).
- [37] Sheikh, U.: *Ph.D. Thesis* (University of the Punjab, Lahore, 2007)
- [38] Achenbach, J.D.: *Wave Propagation in Elastic Solids* (North-Holland Publishing Company, Oxford, 1973).

- [39] Pain, H.J.: *The Physics of Vibrations and Waves* (John Wiley and Sons, Chichester, 2005).

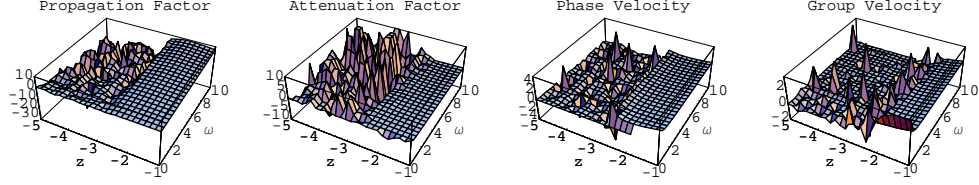


Figure 1: A large region admits normal dispersion of waves moving towards the pair production region.

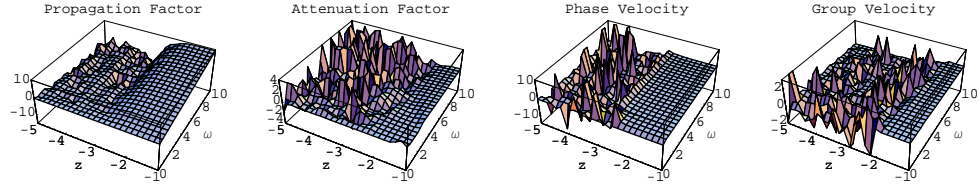


Figure 2: A small region in the neighborhood of the pair production region indicates anomalous dispersion at small angular frequencies. A small region shows the waves are moving towards the event horizon.

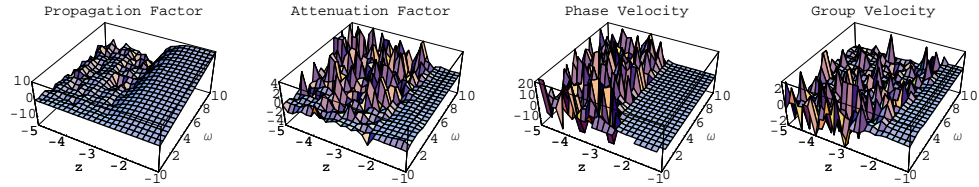


Figure 3: Random dispersion of waves is found. A small region shows that the waves are moving towards the pair production region.

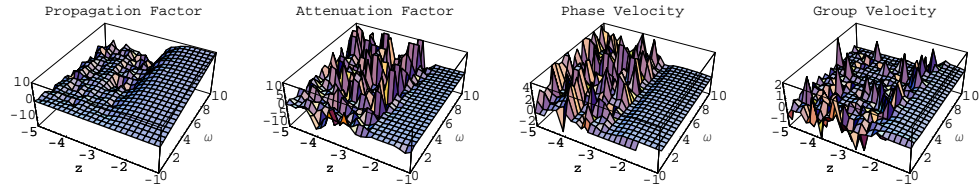


Figure 4: The region near to the pair production region shows anomalous dispersion for the waves moving towards the pair production region.

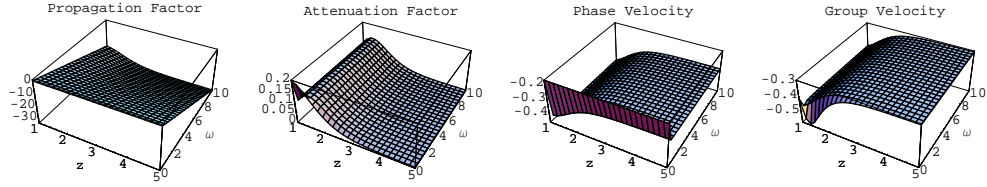


Figure 5: Wave propagation decreases as the waves move towards the pair production region. Small regions admitting normal dispersion are found.

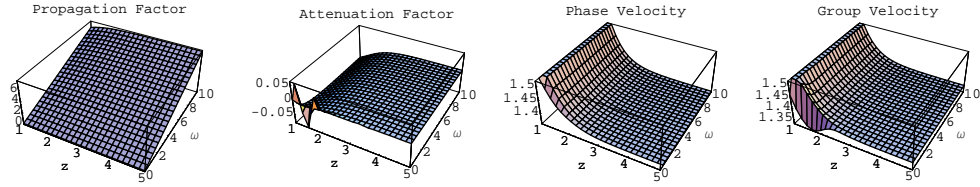


Figure 6: The waves damp as they move away from the pair production region except for the waves with very small angular frequencies. Regions of anomalous dispersion are found for small angular frequencies in the neighborhood of the pair production region.

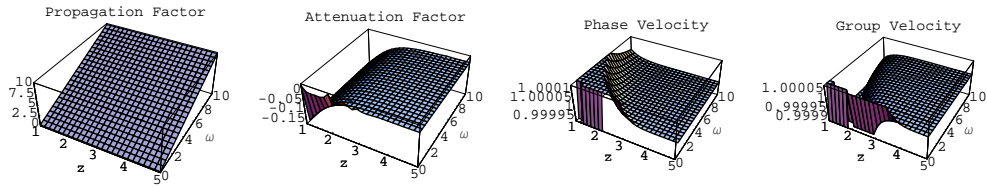


Figure 7: The waves damp while moving away from the pair production region (except for the waves with small angular frequencies). Normal dispersion is found except for the negligible angular frequency waves.

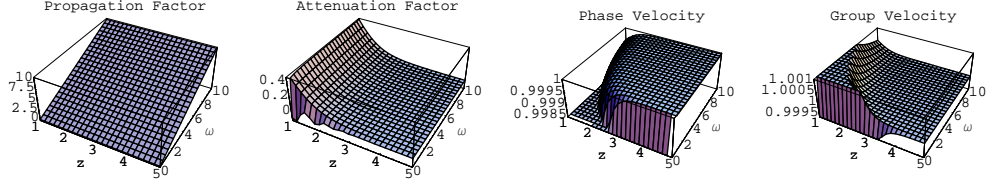


Figure 8: Waves grow as they move away from the pair production region. In most of the region, dispersion is anomalous except for the waves with very small angular frequencies lying between 0.2225 and 5.

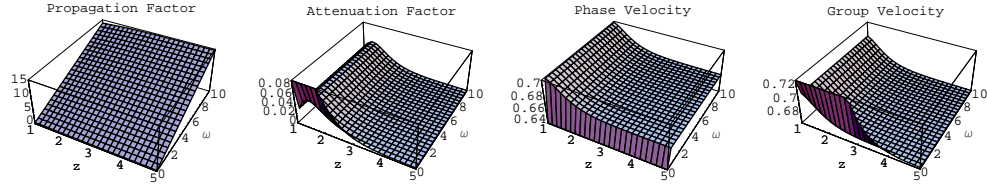


Figure 9: The propagation of waves increases with increasing angular frequency. Waves with small angular frequencies admit normal dispersion.

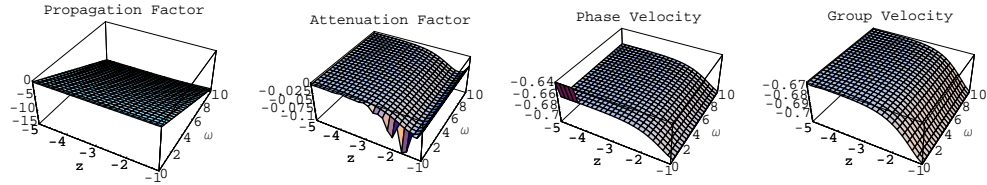


Figure 10: Waves grow and then damp when the value of z increases. This propagation decreases as their angular frequency increases. Dispersion is found to be normal in a small region.

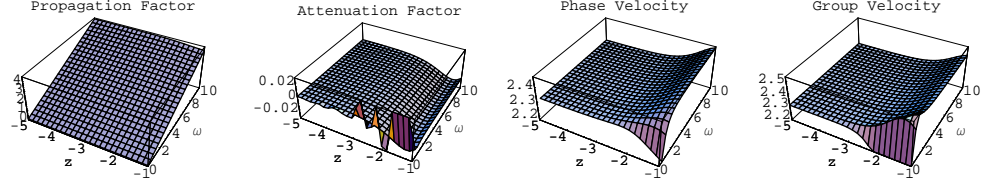


Figure 11: The propagation of waves decreases when the waves move away from the event horizon. Waves damp first and then grow while moving towards the pair production region. Small regions show normal and anomalous dispersion of waves.

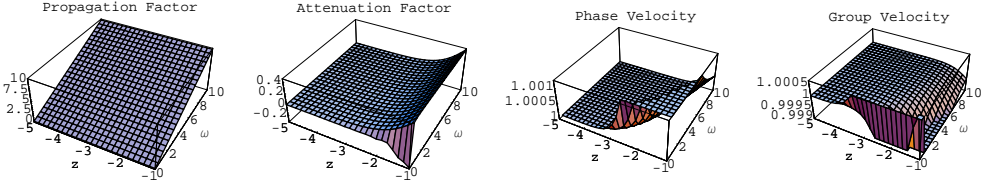


Figure 12: Waves damp as they move towards the pair production region. Random points of normal and anomalous dispersion are found.

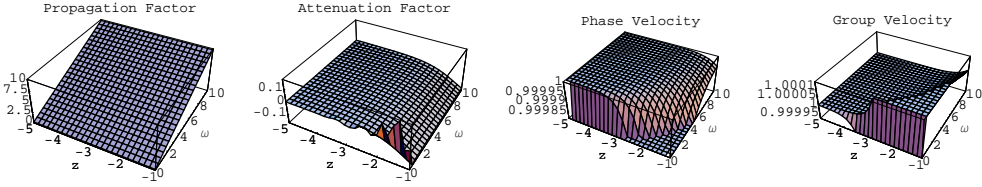


Figure 13: The increase in the angular frequency increases the wave propagation. Waves grow as they move towards the pair production region. A region of normal dispersion is found for small frequency waves.

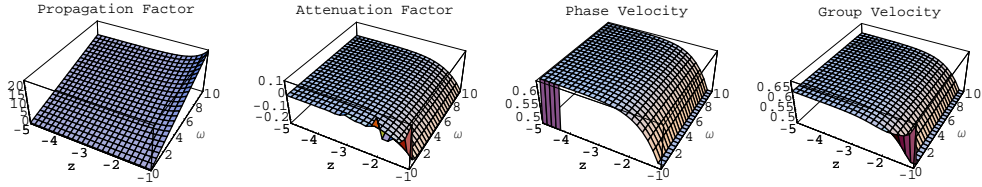


Figure 14: The wave propagation decreases and the waves damp as they move towards the pair production region except for the low angular frequency waves. Small region admitting normal dispersion of waves are identified.

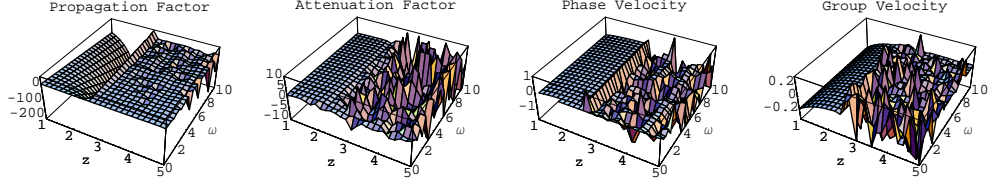


Figure 15: The medium admits a small region for the waves moving towards the pair production region. The wave propagation decreases and then increases as the waves move away from the event horizon. Small regions of normal and anomalous dispersion are found.

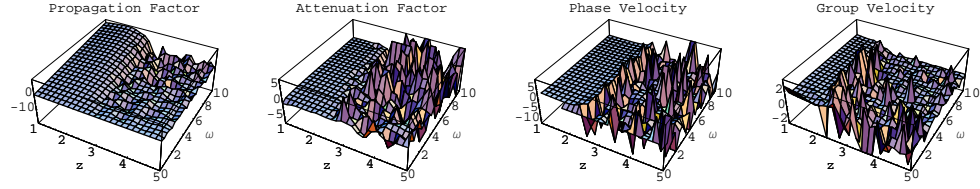


Figure 16: The propagation vector, attenuation factor, phase and group velocity vectors admit random values away from the pair production region. Small regions near the pair production region show normal dispersion.

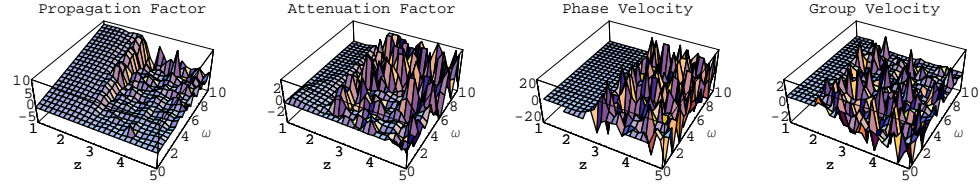


Figure 17: A small region admitting anomalous dispersion of waves moving towards the outer end of the magnetosphere.

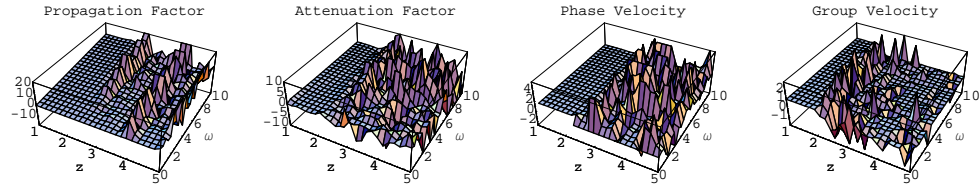


Figure 18: A small region in the neighborhood of the pair production region shows normal dispersion of the low angular frequency waves moving towards the outer end of the magnetosphere.